# New 1,2,3-triazole-linked tetrahydrobenzo[*b*]pyran derivatives: Facile synthesis, biological evaluation and molecular docking study

Published: 21 June 2019

Volume 45, pages 5159–5182, (2019) Cite this article



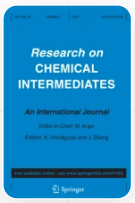


Research on Chemical Intermediates

Aims and scope

Submit manuscript

Smita P. Khare, Tejshri R. Deshmukh, Satish V. Akolkar, Jaiprakash N. Sangshetti, Vijay M. Khedkar & Bapurao B. Shingate



## Abstract

An efficient ultrasound-promoted one-pot three-component synthesis of a series of new 1,2,3-triazole-linked tetrahydrobenzo[*b*]pyran derivatives as antifungal and antioxidant agents using $NaHCO_3$ has been described for the first time. The bioassay result indicates that the compounds **7b**, **7c**, **7i** and **7j** displayed excellent antifungal activity with lower MIC = 12.5 µg/mL than the reference drug miconazole. Most of the compounds from the series showed promising antioxidant activity with lower $IC_{50}$ values in the range 12.47 ± 0.60–16.49 ± 0.44 µg/mL in comparison with butylated hydroxy toluene (BHT). Molecular docking studies revealed that most of the newly synthesized compounds showed

excellent binding affinity with the potential target sterol 14α-demethylase (CYP51). Moreover, in silico adsorption, distribution, metabolism and excretion (ADME) study shows that the derivatives may possess drug like properties for further development of newer therapeutic agents.

## Graphic abstract

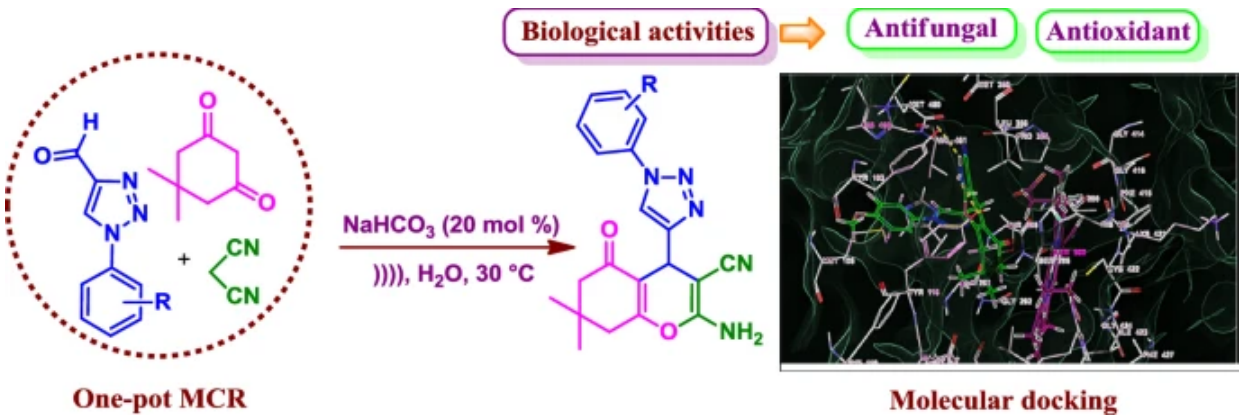




## Introduction

Over the past few decades, invasive fungal infections have remained a major public health threat in critically ill patients [1]. In recent years, incidence of fungal infections has significantly increased in case of immune-compromised individuals due to organ transplant, anticancer chemotherapy, AIDS and burns [2]. Fungal infections in these immunocompromised patients are severe and difficult to treat. However, different classes of chemotherapeutic agents such as polyenes, pyrimidines, allylamines, echinocandins and azoles were used to treat fungal infections with different modes of action including inhibition of ergosterol, chitin, glucan, protein, microtubule and nucleic acid synthesis [3, 4]. Presently, azole-based antifungal agents are used in the treatment of fungal infections. Voriconazole, posaconazole and ravuconazole are the newly introduced antifungal drugs [5]. Despite azoles being the major source of antifungal therapy, increasing use of azole antifungal drugs is resulting in the development of resistance in pathogens [6]. However, development of novel chemical entities remains a key challenge for researchers to achieve improved therapeutic outcomes associated with fungal infections. All the above facts alarm the need for newer azoles with improved efficacy, oral bioavailability, elaborated potency and reduced adverse effect with toxicity.

In recent years, triazoles have been used successfully in the treatment of fungal infections due to their broad therapeutic index. Triazoles inhibit growth and replication of fungi through a mechanism including interaction with cytochrome P450 14α-demethylase (CYP51) which plays a vital role in ergosterol biosynthesis. The CYP51 enzyme catalyzes oxidative removal of the 14α-methyl group of lanosterol by monooxygenase activity [7]. Azoles disrupts this oxidative removal through binding of azole N-4 to the iron protoporphyrin unit of CYP51 which results in depletion of ergosterol and accumulation of 14α-methylated sterol. This affects the membrane fluidity and activity of membrane enzymes which leads to retardation of fungal growth [8].

1,2,3-Triazoles and 4*H*-pyrans are not prevalent in nature, but these class of heterocyclic compounds have garnered outmost relevance not only as biologically active ingredients, but also in the fields of materials and coordination chemistry. 1,2,3-Triazoles have been a fruitful source of inspiration for medicinal chemists for new drug development in the field of drug discovery. Cu-catalysed azide-alkyne 1,3-dipolar cycloaddition is one of the popular routes to obtain 1,2,3-triazoles [9,10,11]. Triazoles are known to possess interesting physicochemical properties along with a broad spectrum of biological activities (Fig. 1) [12,13,14,15].

**Fig. 1**

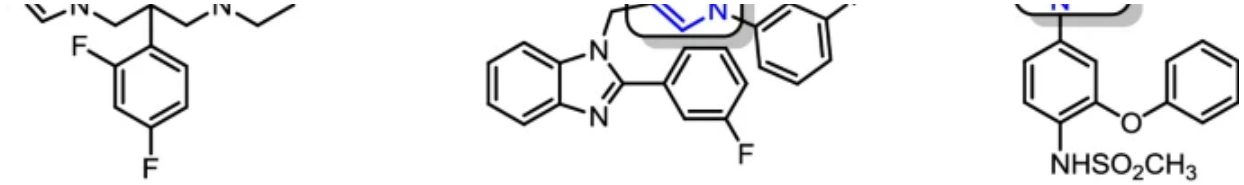


Biologically important synthetic 1,2,3-triazoles

Further, 4*H*-pyran and pyran annulated heterocycles are found in both nature and via synthetic origin and are reported to display diverse pharmaceutical and biological activities [16] such as antibacterial [17], antitubercular [18], anticancer [19], antimicrobial [20], antifungal [21], apoptosis inducer [22], anti-inflammatory [23] and antimalarial activities [24]. Some of the synthetic 2-amino-4*H*-pyran derivatives are shown in Fig. 2. The molecule EPC 2407 is an anticancer drug in phase I of clinical trials with tumor vascular endothelial disrupting activity [19]. Recently, Thanh et al. [25] have reported 1,2,3-triazole-4*H*-chromene-D-glucose conjugates as antibacterial and antifungal agents.

**Fig. 2**

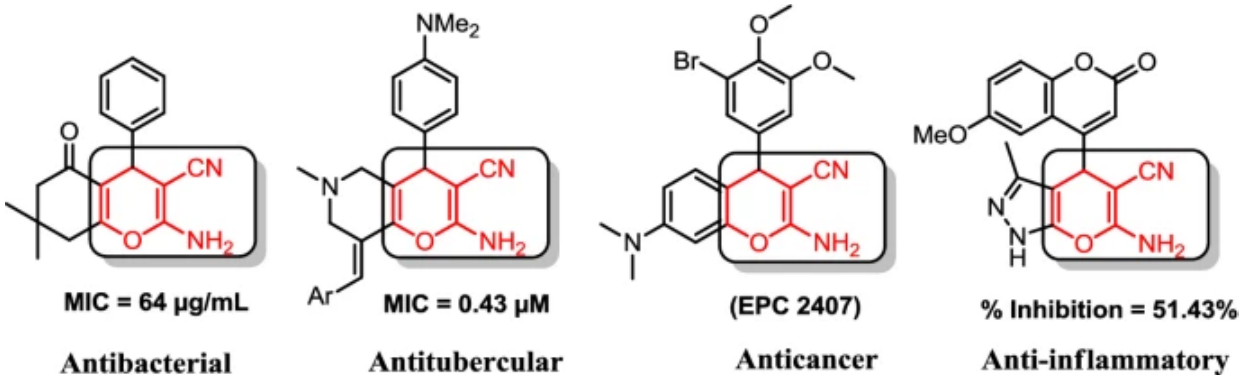


4*H*-Pyran-based biologically active molecules

Owing to the biological significance of 4*H*-pyran and its derivatives, different multicomponent reaction (MCR) strategies have been developed for the synthesis of a diversified 4*H*-pyran molecular scaffold. A recent catalytic system for the synthesis of tetrahydrobenzo[*b*]pyran via one-pot three-component reaction of various aldehydes with dimedone and malononitrile has been achieved by conventional methods, which includes use of lactose [26], β-cyclodextrin [27], per-6-amino-β-cyclodextrin [28],

glycerol [29], nano-$Fe_3O_4$ [30], $I_2$ [31], Tris-hydroxymethylaminomethane (THAM) [32] and $PEG_{1000}$-DAIL [33]. In addition, their synthesis has also been reported by non-conventional protocols such as microwave irradiation, ultrasonic irradiation and ball milling technique [34,35,36,37]. Although most of these methods are efficient with their own merits and demerits, there is still a major scope for introduction of newer, safer, environmentally benign and high-yielding protocols for the synthesis of medicinally important 4*H*-pyran scaffolds.

Designing organic reactions via green chemistry protocol is a key challenge posed to researchers for the development of environmentally benign chemical processes [38]. Multicomponent reactions (MCRs) are a valuable tool that complies with green chemistry principles to generate target molecules with structural diversity in single transformation [39, 40]. Water-mediated MCRs are the ultimate goal of green chemistry because it offers several benefits of green chemistry along with rate acceleration [41]. Furthermore, the use of ultrasonic irradiation as a green source of energy has increased with growing popularity. In comparison with traditional methods, ultrasound offers several advantages such as high yields in shorter reaction time at ambient temperature, and it also differs from traditional energy sources such as heat, light and ionizing radiation. The mechanism of rate enhancement due to sonochemical effects is mainly based on acoustic cavitation phenomenon which includes formation and collapse of bubbles. This process is capable of providing high temperature and pressure in micro-seconds which drives reactions to completion in short times [42]. Surprisingly, methods in the synthesis and bioevaluation of 1,2,3-triazole-linked 2-amino-4*H*-pyran scaffold has not been reported.

Owing to the biological significance of 1,2,3-triazoles, and 4*H*-pyran as discussed above, and in continuation of our earlier research endeavor on MCRs, synthesis and bioevaluation of new heterocyclic compounds [43,44,45,46], we would like to report a simple, efficient, inexpensive, environmentally benign protocol for the synthesis of new 1,2,3-triazole-linked 4*H*-pyran scaffolds and evaluation of their antifungal and antioxidant activity. We have designed and synthesized target molecules based on the molecular hybridization concept [47], which makes it possible to assemble biologically active scaffolds, i.e. triazole-pyran, into a single molecular framework (Fig. 3).

**Fig. 3**

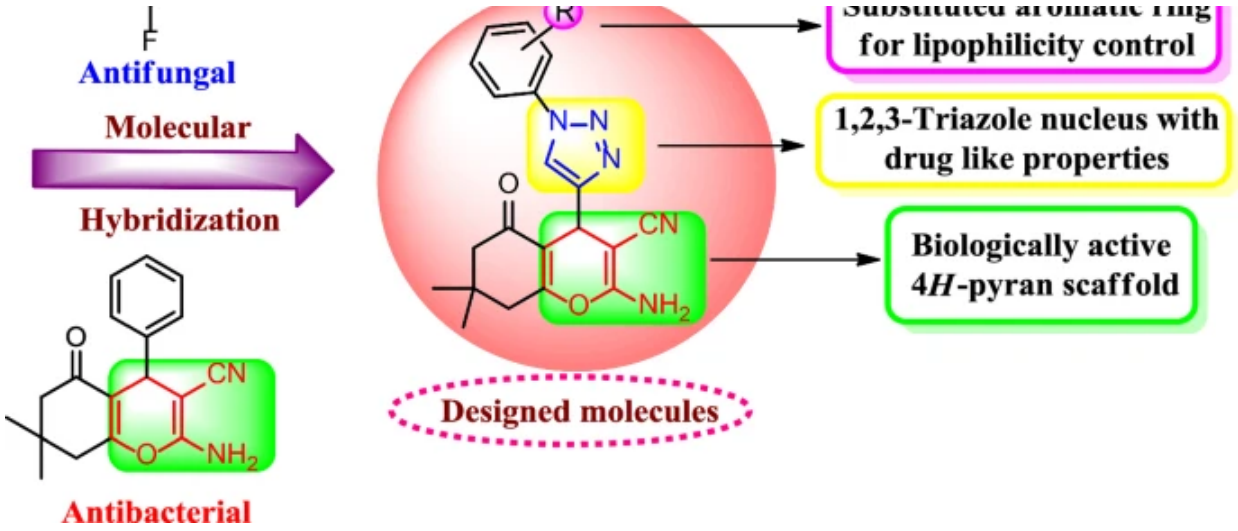


Design strategy for the synthesis of 1,2,3-triazole-linked tetrahydrobenzo[*b*]pyran via molecular hybridization approach

# Experimental

## General

All the solvents and reagents were purchased from commercial suppliers Spectrochem Pvt. Ltd., Sigma Aldrich and Rankem India Ltd. and are used without further purification. All the one-pot reactions were performed using a Citizen (CUB 2.5) ultrasonic cleaner bath working at 40 kHz (constant frequency, 50 W). The progress of each reaction was monitored by ascending thin layer chromatography (TLC) using TLC aluminum sheets, precoated silica gel 60 $F_{254}$ (Merck, Germany) and locating the spots using UV light as the visualizing agent or iodine vapors. Melting points were determined in an open capillary method and are uncorrected. Infrared (IR) spectra were recorded as a neat sample on a Bruker (ALPHA Eco-ATR) FT-IR spectrometer. $^{1}$H NMR spectra were recorded ($CDCl_3$/DMSO-$d_6$/$CDCl_3$ + DMSO-$d_6$) on a Bruker Avance 200 and 400-MHz NMR spectrometer. $^{13}$C NMR spectra were recorded (DMSO-$d_6$/$CDCl_3$ + DMSO-$d_6$) on a Bruker Avance 50 and 100-MHz NMR spectrometer. Mass spectra were recorded on an Agilent 6520 [quadrupole time-of-flight (Q-Tof), high-resolution electrospray ionization mass spectrometry (ESI-HRMS)] and Waters UPLC-TQD (ESI-MS) instrument. Chemical shifts ($\delta$) are reported in parts per million (ppm) using tetramethylsilane (TMS) as an internal standard. The splitting pattern abbreviations are designed as singlet (s); doublet (d); double doublet (dd); triplet (t), broad singlet (bs) and multiplet (m).

## General procedure for the synthesis of 1,2,3-triazole-linked tetrahydrobenzo[*b*]pyran derivatives (7a–j)

## Method A

A mixture of appropriate 1-aryl-1*H*-[1,2,3]triazole-4-carbaldehydes (**4a–j**; 1 mmol), dimedone (**5**; 1 mmol), malononitrile (**6**; 1 mmol) and tetrabutyl ammonium bromide (TBAB) (10 mol%) in water (5 mL) was taken in a 50-mL round-bottomed flask, and the mixture was stirred under reflux condition for an appropriate time. After the completion of the reaction monitored by TLC, the reaction mixture was poured into 20 mL of ice water, and the obtained solid was filtered, washed thoroughly with water, dried and recrystallized from ethanol to afford the pure products (**7a–j**).

## Method B

A mixture of appropriate 1-aryl-1*H*-[1,2,3]triazole-4-carbaldehydes (**4a–j**; 1 mmol), dimedone (**5**; 1 mmol), malononitrile (**6**; 1 mmol) and $NaHCO_3$ (20 mol%) in water (5 mL) was taken in a 50-mL round-bottomed flask, and the mixture was sonicated in a ultrasonic bath working at 40 kHz (constant frequency) at 30 °C for an appropriate time. After the completion of the reaction (monitored by TLC), the reaction mixture was poured into 20 mL of ice water, and the obtained solid was filtered, washed thoroughly with water, dried and recrystallized from ethanol to afford the pure products (**7a–j**) in excellent yields.

## 2-Amino-7,7-dimethyl-5-oxo-4-(1-phenyl-1*H*-1,2,3-triazol-4-yl)-5,6,7,8-tetrahydro-4*H* chromene-3-carbonitrile (7a)

Mp: 222–224 °C. IR $\nu_{max}$ ($cm^{-1}$): 3338, 3293 ($NH_2$), 2185 (CN), 1651 (C=C vinyl nitrile), 1599 (C=C aromatic). $^1$H NMR (400 MHz, $CDCl_3$, $\delta$ ppm): 1.12 (s, 3H), 1.14 (s, 3H), 2.29–2.56 (m, 4H), 4.72 (s, 1H, H-4), 4.85 (s, 2H, $NH_2$), 7.43 (t, 1H, $J$ = 8 Hz), 7.52 (t, 2H, $J$ = 8 Hz), 7.74 (d, 2H, $J$ = 8 Hz), 8.00 (s, 1H, triazolyl-H). $^{13}$C NMR (100 MHz, $CDCl_3$, $\delta$ ppm): 27.1, 27.8, 28.8, 32.4, 40.7, 50.6 (C–CN), 60.6, 112.1, 119.5, 120.5, 128.6, 129.7, 158.6, 162.8 (C–$NH_2$), 196.4 (C=O). ES–MS: calculated for $C_{20}H_{19}N_5O_2$ [M + H]$^+$, 362.1617, found: 362.

## 2-Amino-4-(1-(4-methylphenyl)-1*H*-1,2,3-triazol-4-yl)-7,7-dimethyl-5-oxo-5,6,7,8-tetrahydro-4*H*-chromene-3-carbonitrile (7b)

Mp: 220–222 °C. IR $\nu_{max}$ ($cm^{-1}$): 3323, 3255 ($NH_2$), 2184 (CN), 1644 (C=C vinyl nitrile), 1597 (C=C aromatic). $^1$H NMR (400 MHz, $CDCl_3$ + DMSO-$d_6$, $\delta$ ppm): 1.11 (s, 3H), 1.13 (s, 3H), 2.22–2.42 (m, 4H), 2.42 (s, 3H), 4.62 (s, 1H, H-4), 6.29 (bs, 2H, $NH_2$), 7.32 (d, 2H, $J$ = 8 Hz), 7.63 (d, 2H, $J$ = 8 Hz), 8.05 (s, 1H, triazolyl-H). $^{13}$C NMR (100 MHz, $CDCl_3$ + DMSO-$d_6$, $\delta$ ppm): 25.8, 32.1, 32.4, 33.6, 37.1, 55.3 (C–CN), 116.5, 124, 124.1, 124.8, 135, 139.5, 143.2, 154.7, 164.1, 167.7 (C–$NH_2$), 201 (C=O). HRMS: calculated for $C_{21}H_{21}N_5O_2$ [M + H]$^+$, 376.1773, found: 376.1788.

## 2-Amino-4-(1-(4-methoxyphenyl)-1*H*-1,2,3-triazol-4-yl)-7,7-dimethyl-5-oxo-5,6,7,8-tetrahydro-4*H*-chromene-3-carbonitrile (7c)

Mp: 217–219 °C. IR $\nu_{max}$ ($cm^{-1}$): 3333, 3257 ($NH_2$), 2184 (CN), 1667 (C=C vinyl nitrile), 1593 (C=C aromatic). $^1H$ NMR (200 MHz, $CDCl_3$ + DMSO-$d_6$, $\delta$ ppm): 1.04 (s, 3H), 1.07 (s, 3H), 2.12–2.40 (m, 4H), 3.84 (s, 3H), 4.48 (s, 1H, H-4), 7.06 (s, 2H, $NH_2$), 7.14 (d, 1H, $J$ = 8 Hz), 7.30 (d, 1H, $J$ = 8 Hz), 7.46–7.55 (m, 1H), 7.62 (d, 1H, $J$ = 8 Hz), 8.18 (s, 1H, triazolyl-H). $^{13}C$ NMR (50 MHz, $CDCl_3$ + DMSO-$d_6$, $\delta$ ppm): 27, 27.1, 28.4, 32, 50, 55.3 ($OCH_3$), 56.5 (C–CN), 111.2, 114.6, 119.3, 119.6, 121.2, 130.1, 150.1, 159.1, 162.7 (C–$NH_2$), 195.4 (C=O). HRMS: calculated for $C_{21}H_{21}N_5O_3$ [M + H]$^+$, 392.1723, found: 392.1730.

## 2-Amino-4-(1-(3-methoxyphenyl)-1*H*-1,2,3-triazol-4-yl)-7,7-dimethyl-5-oxo-5,6,7,8-tetrahydro-4*H*-chromene-3-carbonitrile (7d)

Mp: 208–210 °C. IR $\nu_{max}$ ($cm^{-1}$): 3364, 3310 ($NH_2$), 2182 (CN), 1654 (C=C vinyl nitrile), 1500 (C=C aromatic). $^1H$ NMR (200 MHz, DMSO-$d_6$, $\delta$ ppm): 1.03 (s, 3H), 1.06 (s, 3H), 2.15–2.31 (m, 4H), 3.86 (s, 3H), 4.47 (s, 1H, H-4), 7.10 (s, 2H, $NH_2$), 7.38–7.60 (m, 4H), 8.69 (s, 1H, triazolyl-H). $^{13}C$ NMR (50 MHz, DMSO-$d_6$, $\delta$ ppm): 26.7, 27.1, 28.4, 31.9, 49.9, 55.6 ($OCH_3$), 56.3 (C–CN), 105.2, 111, 111.6, 114.2, 119.7, 130.8, 137.6, 150.5, 159, 160.2, 163.1 (C–$NH_2$), 195.8 (C=O). ES–MS: calculated for $C_{21}H_{21}N_5O_3$ [M + H]$^+$, 392.1723, found: 392.

## 2-Amino-4-(1-(2-methoxyphenyl)-1*H*-1,2,3-triazol-4-yl)-7,7-dimethyl-5-oxo-5,6,7,8-tetrahydro-4*H*-chromene-3-carbonitrile (7e)

Mp: 210–212 °C. IR $\nu_{max}$ ($cm^{-1}$): 3361, 3300 ($NH_2$), 2185 (CN), 1648 (C=C vinyl nitrile), 1598 (C=C aromatic). $^1H$ NMR (200 MHz, DMSO-$d_6$, $\delta$ ppm): 1.07 (s, 3H), 1.09 (s, 3H), 2.13–2.32 (m, 4H), 3.84 (s, 3H), 4.50 (s, 1H, H-4), 6.92 (s, 2H, $NH_2$), 7.06 (d, 2H, $J$ = 6 Hz), 7.77 (d, 2H, $J$ = 6 Hz), 8.40 (s, 1H, triazolyl-H). $^{13}C$ NMR (50 MHz, DMSO-$d_6$, $\delta$ ppm): 26.6, 27, 28.5, 31.9, 49.9, 56.1 ($OCH_3$), 56.5 (C–CN), 111.3, 113.1, 119.7, 120.9, 123.2, 125.2, 125.7, 130.4, 149.1, 151.1, 159.1, 163.1 (C–$NH_2$), 195.7 (C=O). ES–MS: calculated for $C_{21}H_{21}N_5O_3$ [M + H]$^+$, 392.1723, found: 392.

## 2-Amino-4-(1-(4-chlorophenyl)-1*H*-1,2,3-triazol-4-yl)-7,7-dimethyl-5-oxo-5,6,7,8-tetrahydro-4*H*-chromene-3-carbonitrile (7f)

Mp: 221–223 °C. IR $\nu_{max}$ ($cm^{-1}$): 3456, 3322 ($NH_2$), 2184 (CN), 1677 (C=C vinyl nitrile), 1497 (C=C aromatic). $^1H$ NMR (200 MHz, DMSO-$d_6$, $\delta$ ppm): 1.02 (s, 3H), 1.06 (s, 3H), 2.11–2.42 (m, 4H), 4.47 (s, 1H, H-4), 7.10 (s, 2H, $NH_2$), 7.66 (d, 2H, $J$ = 8 Hz), 7.95 (d, 2H, $J$ = 8 Hz), 8.70 (s, 1H, triazolyl-H). $^{13}C$ NMR (50 MHz, DMSO-$d_6$, $\delta$ ppm): 26.8, 27.1, 28.3, 31.9, 49.9, 56.2 (C–CN), 110.9, 119.7, 121.3, 129.8, 132.7, 135.4, 150.8, 159, 163.1 (C–$NH_2$), 195.8 (C=O). ES–MS: calculated for $C_{20}H_{18}ClN_5O_2$ [M + H]$^+$, 396.1227, found: 396.

## 2-Amino-4-(1-(3-chlorophenyl)-1*H*-1,2,3-triazol-4-yl)-7,7-dimethyl-5-oxo-5,6,7,8-tetrahydro-4*H*-chromene-3-carbonitrile (7g)

Mp: 209–211 °C. IR $\nu_{max}$ ($cm^{-1}$): 3352, 3306 ($NH_2$), 2192 (CN), 1665 (C=C vinyl nitrile), 1488 (C=C aromatic). $^1$H NMR (200 MHz, DMSO-$d_6$, $\delta$ ppm): 1.03 (s, 3H), 1.06 (s, 3H), 2.12–2.42 (m, 4H), 4.48 (s, 1H, H-4), 7.12 (s, 2H, $NH_2$), 7.5–7.67 (m, 2H), 7.92 (d, 1H, $J$ = 6 Hz), 8.04 (s, 1H), 8.76 (s, 1H, triazolyl-H). $^{13}$C NMR (50 MHz, DMSO-$d_6$, $\delta$ ppm): 26.8, 27.1, 28.3, 31.9, 49.9, 56.2 (C–CN), 110.9, 118.2, 119.4, 119.6, 119.8, 128.3, 131.6, 134.2, 137.6, 150.8, 159.1, 163.2 (C–$NH_2$), 195.8 (C=O). ES–MS: calculated for $C_{20}H_{18}ClN_5O_2$ $[M + H]^+$, 396.1227, found: 396.

## 2-Amino-4-(1-(4-nitrophenyl)-1*H*-1,2,3-triazol-4-yl)-7,7-dimethyl-5-oxo-5,6,7,8-tetrahydro-4*H*-chromene-3-carbonitrile (7h)

Mp: 224–226 °C. IR $\nu_{max}$ ($cm^{-1}$): 3439, 3322 ($NH_2$), 2180 (CN), 1674 (C=C vinyl nitrile), 1589 (C=C aromatic). $^1$H NMR (200 MHz, DMSO-$d_6$, $\delta$ ppm): 1.03 (s, 3H), 1.07 (s, 3H), 2.11–2.43 (m, 4H), 4.51 (s, 1H, H-4), 7.15 (s, 2H, $NH_2$), 8.23 (d, 2H, $J$ = 8 Hz), 8.45 (d, 2H, $J$ = 8 Hz), 8.92 (s, 1H, triazolyl-H). $^{13}$C NMR (50 MHz, DMSO-$d_6$, $\delta$ ppm): 26.8, 27.2, 28.3, 32, 49.9, 56 (C–CN), 110.83, 119.6, 120.2, 125.6, 140.8, 146.5, 151.3, 159.1, 163.2 (C–$NH_2$), 195.7 (C=O). ES–MS: calculated for $C_{20}H_{18}N_6O_4$ $[M + H]^+$, 407.1468, found: 407.

## 2-Amino-4-(1-(3-nitrophenyl)-1*H*-1,2,3-triazol-4-yl)-7,7-dimethyl-5-oxo-5,6,7,8-tetrahydro-4*H*-chromene-3-carbonitrile (7i)

Mp: 207–209 °C. IR $\nu_{max}$ ($cm^{-1}$): 3314, 3252 ($NH_2$), 2189 (CN), 1656 (C=C vinyl nitrile), 1595 (C=C aromatic). $^1$H NMR (200 MHz, DMSO-$d_6$, $\delta$ ppm): 1.03 (s, 3H), 1.07 (s, 3H), 2.11–2.43 (m, 4H), 4.50 (s, 1H, H-4), 7.14 (s, 2H, $NH_2$), 7.89 (t, 1H, $J$ = 8.2 Hz), 8.31 (d, 1H, $J$ = 8 Hz), 8.42 (d, 1H, $J$ = 8 Hz), 8.73 (s, 1H), 8.96 (s, 1H, triazolyl-H). ES–MS: calculated for $C_{20}H_{18}N_6O_4$ $[M + H]^+$, 407.1468, found: 407.

## 2-Amino-4-(1-(2-nitrophenyl)-1*H*-1,2,3-triazol-4-yl)-7,7-dimethyl-5-oxo-5,6,7,8-tetrahydro-4*H*-chromene-3-carbonitrile (7j)

Mp: 204–206 °C. IR $\nu_{max}$ ($cm^{-1}$): 3398, 3229 ($NH_2$), 2177 (CN), 1641 (C=C vinyl nitrile), 1535 (C=C aromatic). $^1$H NMR (200 MHz, DMSO-$d_6$, $\delta$ ppm): 1.01 (s, 3H), 1.06 (s, 3H), 2.12–2.40 (m, 4H), 4.50 (s, 1H, H-4), 7.13 (s, 2H, $NH_2$), 7.77–7.97 (m, 3H), 8.18 (d, 1H, $J$ = 8 Hz), 8.49 (s, 1H, triazolyl-H). $^{13}$C NMR (50 MHz, DMSO-$d_6$, $\delta$ ppm): 26.6, 26.9, 28.4, 32, 49.9, 56.0 (C–CN), 111.2, 119.6, 122.8, 125.4, 127.1, 130.9, 134.2, 143.9, 150.3, 159.3, 163.1, (C–$NH_2$), 195.5 (C=O). ES–MS: calculated for $C_{20}H_{18}N_6O_4$ $[M + H]^+$, 407.1468, found: 407.

# Experimental method for biological activity

## In vitro antifungal activity

Antifungal activity was determined by standard agar dilution method as per CLSI (formerly, NCCLS) guidelines [48]. The synthesized compounds and standard miconazole were dissolved in DMSO solvent. The medium yeast nitrogen base was dissolved in phosphate buffer of pH 7, and it was autoclaved at 110 °C for 10 min. With each set, a growth control without the antifungal agent and solvent control DMSO were included. The fungal strains were freshly subcultured onto Sabouraud dextrose agar (SDA) and incubated at 25 °C for 72 h. The fungal cells were suspended in sterile distilled water and diluted to get 105 cells/mL. Ten microliters of standardized suspension was inoculated onto the control plates and the media incorporated with the antifungal agents. The inoculated plates were incubated at 25 °C for 48 h. The readings were taken at the end of 48 and 72 h. The minimum inhibitory concentration (MIC) was the lowest concentration of drug preventing growth of macroscopically visible colonies on drug-containing plates when there was visible growth on the drug-free control plates.

## DPPH radical scavenging activity

Antioxidant activity of the synthesized compounds has been assessed in vitro by the 1,1-diphenyl-2-picrylhydrazyl (DPPH) radical scavenging assay [49], and the results were compared with standard synthetic antioxidant butylated hydroxy toluene (BHT). The hydrogen atom or electron donation ability of the compounds were measured from the bleaching of the purple-colored methanol solution of DPPH. The spectrophotometric assay uses the stable radical DPPH as a reagent. 1 mL of various concentrations of the test compounds (5, 10, 25, 50 and 100 mg/mL) in methanol was added to 4 mL of 0.004% (w/v) methanol solution of DPPH. After a 30-min incubation period at room temperature, the absorbance was measured against a blank at 517 nm. The percent inhibition (I%) of free radical production from DPPH was calculated by the following equation;

$$\% \;{\text{of}}\;{\text{scavenging}} = \left[ {\left( {{\text{A}}\;{\text{control}} - {\text{A}}\;{\text{sample}}} \right) / {\text{A}}\;{\text{blank}}} \right] \times 100$$

where ‘A control’ is the absorbance of the control reaction (containing all reagents except the test compound) and ‘A sample’ is the absorbance of the test compound. Tests were carried out in triplicate.

## Computational study

### Molecular docking

Molecular docking study was carried out using the standard protocol integrated in the Grid-based

LIgand Docking with Energetics (GLIDE) program incorporated in the Schrodinger molecular modeling package (Schrodinger, LLC, New York, NY, USA, 2015) to predict the binding modes of 1,2,3-triazole-linked tetrahydrobenzo[*b*]pyran derivatives (**7a–j**) into the active site of sterol 14α-demethylase (CYP51) enzyme [50]. The workflow involves selection of enzyme and its preprocessing, identification and generation of receptor grid, building and geometry optimization of ligand 3D structures, docking, visualization and analysis of binding mode. The X-ray crystal structure of sterol 14α-demethylase (CYP51) complexed with its inhibitor fluconazole (PDB code: 3KHM) was obtained from the RCSB Protein Data Bank (PDB) [51]. The enzyme-inhibitor complex was refined using the *protein preparation wizard* applying the OPLS-2005 force field which includes deleting the crystallographically observed water molecules (as they not were found to be conserved in the interaction with the enzyme); adding the missing hydrogens/side chain atoms corresponding to pH 7.0 considering the appropriate ionization states for the acidic as well as basic amino acid residues; assignment of appropriate charge and protonation state to the obtained structure; and finally energy minimization of the obtained structure until the average root mean square deviation (RMSD) reached 0.3 Å. The 3D structures of the ligand (**7a–j**) to be docked were sketched in the *build* panel of Maestro and then optimized by running the *Ligand Preparation* protocol and the resulting structures were then subjected to energy minimization until their average reached 0.001 Å. Next, using the *receptor grid generation* panel, the shape and properties of the active site of the CYP51 enzyme were defined for which a grid box of 10 × 10 × 10-Å dimensions centered on the centroid of the co-crystallized ligand (serving as the reference coordinate to signify the active site for the inhibitor) was generated which was sufficient to explore a larger space of the enzyme cavity. Using this setup, docking was carried out to gauze the binding affinities of the title compounds against the defined active site of CYP51 using the extra precision (XP) GLIDE scoring function. The output files generated in the form of the docking poses were visualized and analyzed for the most significant interactions with the residues lining the active site using the Maestro's Pose Viewer utility. The output files (i.e. docking poses) were visualized and analyzed using the Maestro's Pose Viewer for the most significant interactions with the residues lining the active site.

# Results and discussion

## Chemistry

We have attempted one-pot three-component synthesis of new 1,2,3-triazole-linked tetrahydrobenzo[*b*]pyran derivatives, based on molecular hybridization strategy. Initially, the preparation of triazolyl aldehydes (**4a–j**) was carried out according to the method reported in the literature [52], from the commercially available anilines (**1a–j**) via click chemistry approach (Scheme 1).

**Scheme 1**

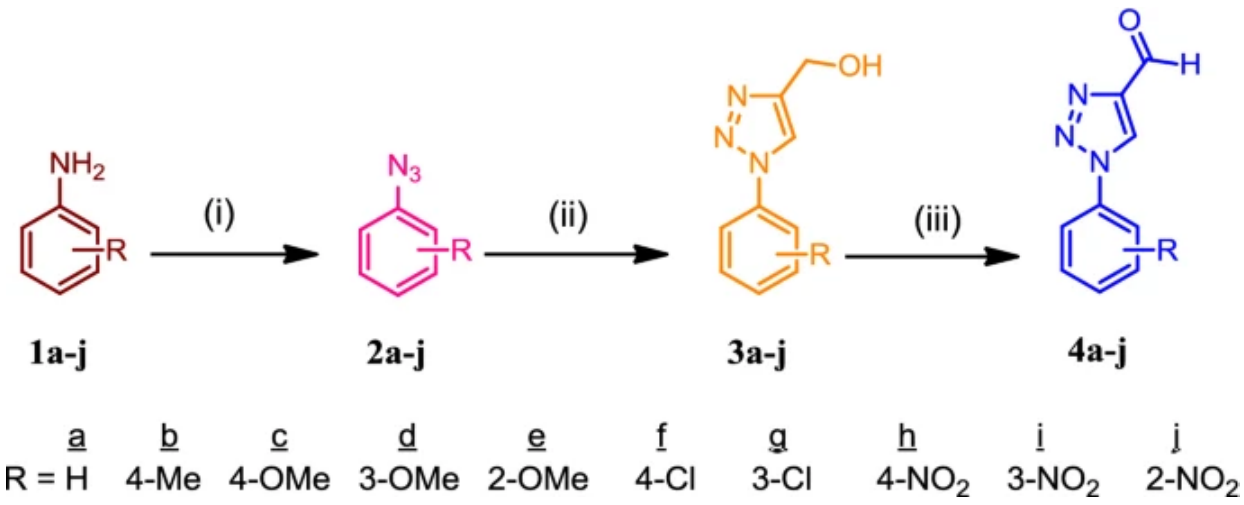


Synthetic route for triazolyl aldehydes (**4a–j**). Reagents and conditions: (i) $NaNO_2$, HCl (10%); $NaN_3$, 1–2 h, 0 °C; (ii) propargyl alcohol, $CuSO_4{\cdot}5H_2O$, sodium ascorbate, *tert*-BuOH-$H_2O$ (1:1), 24–48 h, rt; (iii) Collins reagent ($CrO_3{\cdot}2Py$, $CH_2Cl_2$), 3–6 h, rt

Following the successful applications of triazolyl aldehydes for the synthesis of biologically active heterocyclic scaffolds [52,53,54], we were interested in exploring the use of triazolyl aldehydes in one-pot multicomponent synthesis of diversely functionalized pyran derivatives. At the first stage of our investigation, for the synthesis of triazole-linked tetrahydrobenzo[*b*]pyran, the reaction of triazolyl aldehyde (**4a**), dimedone (**5**) and malononitrile (**6**) was chosen as a model reaction (Scheme 2).

**Scheme 2**

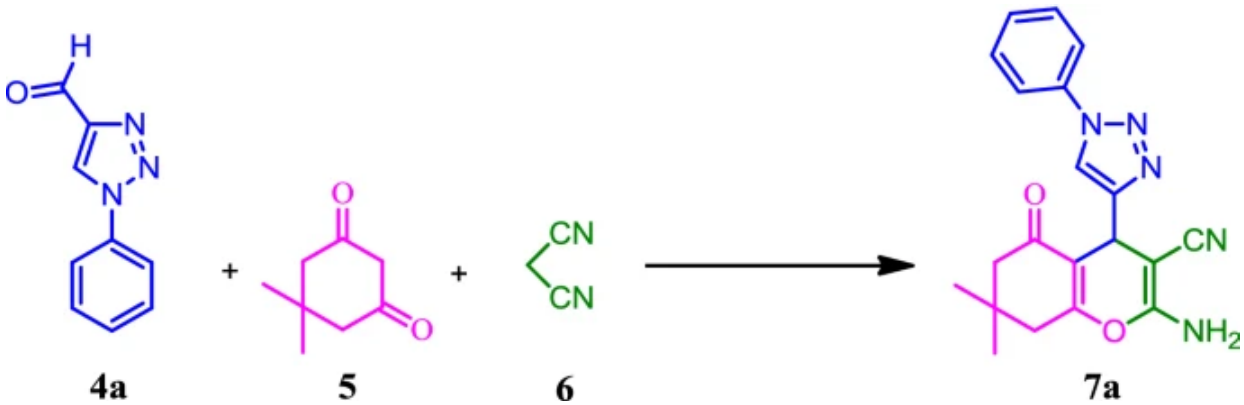


Model reaction

In an initial attempt, the model reaction was performed by using tetrabutyl ammonium bromide (TBAB) as a catalyst in water under reflux condition for 25 min afforded the 1,2,3-triazole-incorporated tetrahydrobenzo[*b*]pyran (**7a**) in 86% yield. TBAB is inexpensive, readily available and used for many organic transformations [55,56,57,58]. Furthermore, to know the scope and efficiency of the above methodology, synthesis of various 1,2,3-triazole-linked tetrahydrobenzo[*b*]pyrans (**7b–j**) was also carried out using TBAB in water under reflux condition for 25–30 min (Scheme 4, Method A), and the obtained results are illustrated in Table 2 (Method A). It is evident from Table 2 (Method A), the results are not satisfactory in terms of reaction time and the yields (76–88%).

In our further attempt to develop greener synthetic protocol and to establish the optimum reaction conditions for the synthesis of the same 1,2,3-triazole-linked tetrahydrobenzo[*b*]pyran derivatives (**7a–j**), the model reaction (Scheme 2) was performed using various inorganic bases such as $K_2CO_3$, $Na_2CO_3$ and $NaHCO_3$ in water as a solvent under ultrasonic irradiation (40 kHz) at 30 °C, and the results are summarized in Table 1. At the preliminary stage, the model reaction was carried out in the absence of catalyst under the same reaction parameters. It was observed that the reaction proceeded to the Knoevenagel product (reaction between **4a** and **6**), and the desired product **7a** was not obtained even after prolonged reaction time (Table 1, entry 1). The reaction was performed by using $K_2CO_3$ (10 and 20 mol%) under the similar reaction parameters, and the desired product **7a** was obtained in 76 and 82% yield, respectively (Table 1, entries 2, 3). Furthermore, with the use of $Na_2CO_3$ (10 mol%), the product **7a** was obtained in 80% yield (Table 1, entry 4). Whereas, increasing the concentration of $Na_2CO_3$ up to 20 mol%, the product **7a** was obtained in 85% yield (Table 1, entry 5). Finally, the reaction was performed by using $NaHCO_3$ (10 mol%); surprisingly, the desired product **7a** was obtained in excellent yield (86%) in shorter reaction time (Table 1, entry 6). Therefore, it was observed that, in comparison with other base catalyst, $NaHCO_3$ has been found to be an efficient catalyst which offers maximum yield in short reaction time. Further, to determine the optimal amount of $NaHCO_3$, the model reaction was subsequently tested for different concentrations, viz. 5, 15, 20 and 25 mol% (Table 1, entries 7–10). Using less than 20 mol% of $NaHCO_3$, good yield (80–94%) of the product **7a** was obtained (Table 1, entries 6–8).

**Table 1 Optimization of the reaction conditions for the preparation of 7a**

It was evident that 20 mol% of $NaHCO_3$ was adequate to obtain optimum yield in short reaction time (Table 1, entry 9). It was observed that no further improvement in the yield was observed with 25 mol% of $NaHCO_3$ (Table 1, entry 10). However, no further increase in the yield was observed by

using 20 and 25 mol% of catalyst with extended reaction time (Table 1, entries 11–12). Finally, to determine the scope of ultrasonic irradiation, the model reaction was performed without ultrasonic irradiation in the presence of 20 mol% $NaHCO_3$ at 30 °C (Table 1, entry 13), and it was observed that the desired product was obtained in trace amount. The above results signify that under ultrasonic condition, 20 mol% of $NaHCO_3$ is the optimum catalyst loading in terms of yield and reaction time. According to the obtained results, 20 mol% of $NaHCO_3$ in water under ultrasonic irradiation (40 kHz) at 30 °C was developed as the optimized reaction conditions.

The formation of the compound **7a** was confirmed by IR, $^1$H NMR, $^{13}$C NMR and mass spectral analysis. In the IR spectrum of compound **7a**, the absorption bands at 3293 and 2185 $cm^{-1}$ appear due to corresponding $NH_2$ and CN groups. In the $^1$H NMR spectrum of compound **7a**, characteristic singlet peaks appearing at $\delta$ 4.72, 4.85 and 8.00 ppm are due to corresponding H-4 (4*H*-pyran ring), $NH_2$ and triazolyl proton. In the $^{13}$C NMR spectrum of compound **7a**, the characteristic signal was observed at $\delta$ 32.4 ppm with respect to the stereogenic methine carbon of the 4*H*-pyran ring. Furthermore, formation of the compound **7a** was confirmed by mass spectrum with a calculated $[M + H]^+$ at 362.1617 and observed at 362.

A plausible mechanism for the synthesis of 1,2,3-triazole-linked tetrahydrobenzo[*b*]pyrans by using $NaHCO_3$ as a base is depicted in Scheme 3. As the initial step, malononitrile is deprotonated by base, and, subsequently, Knoevenagel condensation occurs between malononitrile and triazolyl aldehyde to form Knoevenagel reaction product **I** as a first intermediate. In the next step, dimedone (activated by base) undergoes Michael addition reaction with **I** to afford Michael addition product **II**. At the final step, **II** undergoes intramolecular cyclization through nucleophilic attack on the cyano group to afford intermediate **III** with which further tautomerization affords final product **IV**.

**Scheme 3**

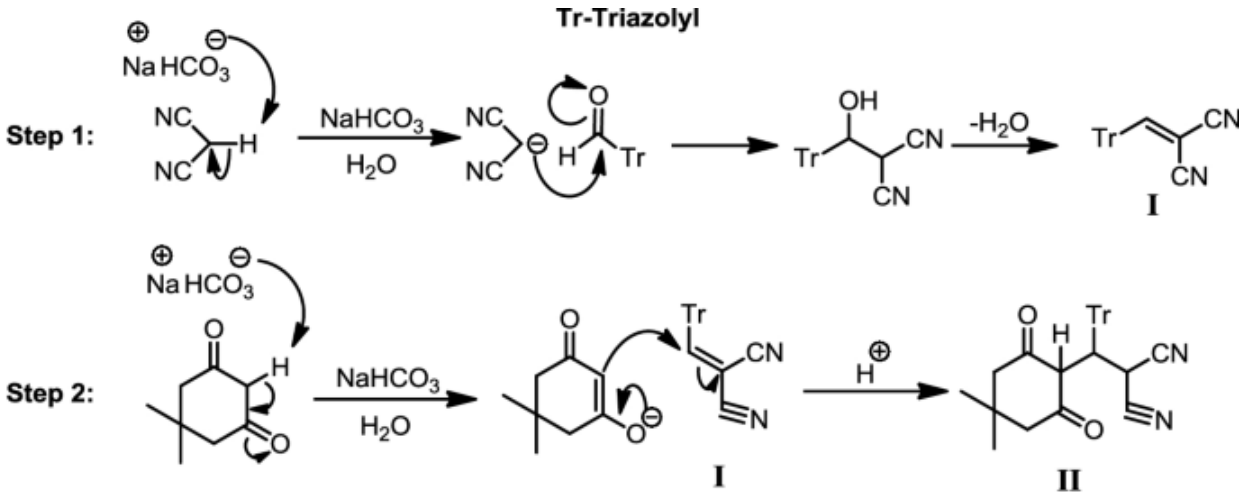

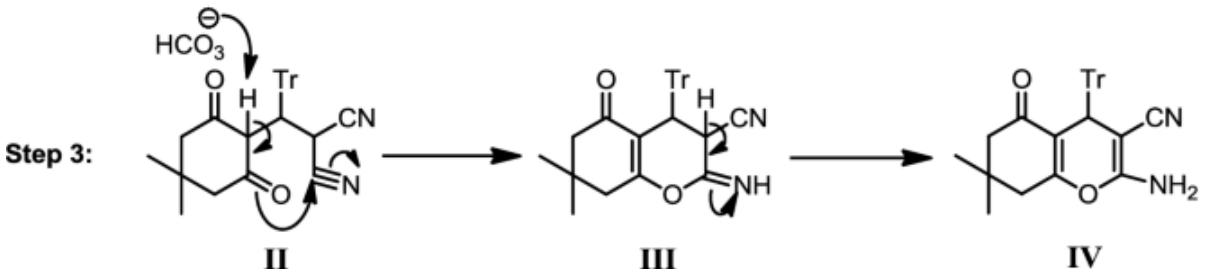


Plausible mechanism for the synthesis of 1,2,3-triazole-linked tetrahydrobenzo[*b*]pyran

Prompted by these promising results, to explore the scope and efficiency of the present green methodology, the optimized reaction conditions were developed for other derivatives of triazolyl aldehydes (**4b–j**; Scheme 4, Method B), and the obtained results are summarized in Table 2 (Method B).

**Scheme 4**

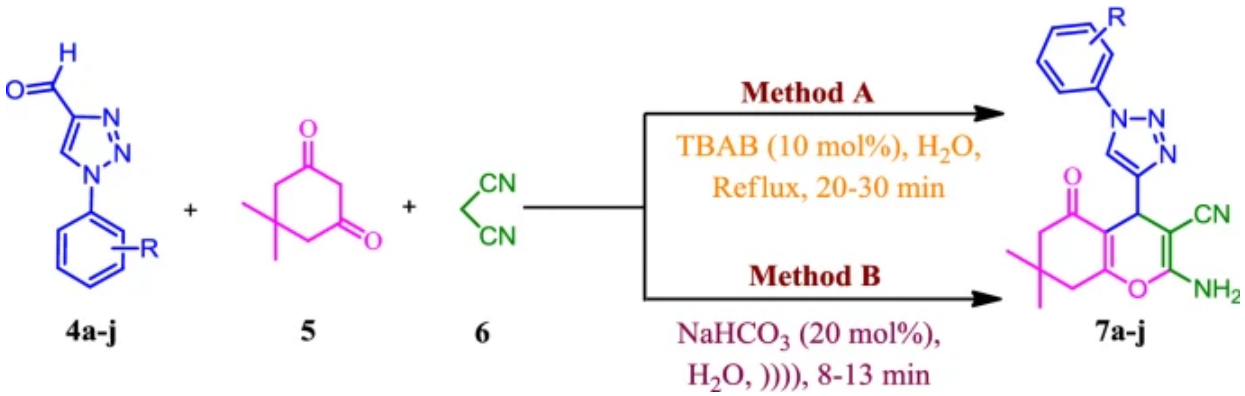


Synthesis of 1,2,3-triazole-linked tetrahydrobenzo[*b*]pyran derivatives (**7a–j**)

**Table 2 Three-component synthesis of 1,2,3-triazole-linked tetrahydrobenzo[*b*]pyran derivatives (7a–j)**

It has been observed from Table 2 (Method B), the reaction conditions work successfully for electron-donating and electron-withdrawing groups (−Me, −OMe, −Cl and $-NO_2$) on triazolyl aldehydes, and corresponding products were obtained in good to excellent yields within shorter reaction time.

# Biological assay

## In vitro antifungal activity

In vitro antifungal activity of all the compounds **7a–j** were evaluated against five human pathogenic fungal strains. Minimum inhibitory concentration (MIC) values were determined by standard agar dilution method. DMSO was used as solvent control, and antifungal activity was compared with standard drug miconazole, and the results are summarized in Table 3.

**Table 3 In vitro antifungal and antioxidant activity of synthesized compounds 7a–j**

From Table 3, it is observed that most of the newly synthesized compounds among the series exhibited good to excellent antifungal activity against nearly all the tested fungal strains. Among the 1,2,3-triazole-linked tetrahydrobenzo[*b*]pyran derivatives (**7a–j**), compounds **7a**, **7b**, **7c**, **7d**, **7i** and **7j** displayed prominent antifungal activity against most of the tested fungal strains. Compounds **7b**, **7c** and **7j** exhibited excellent antifungal activity with MIC = 12.5 µg/mL and were found to be more potent than miconazole against *Candida albicans*. The compounds **7d** and **7i** were found to be equipotent to miconazole against the *C. albicans* with MIC = 25 µg/mL. Compounds **7c** and **7i** were found to be more active than miconazole against *Fusarium oxysporum* with MIC = 12.5 µg/mL. Compounds **7b** and **7j** exhibited equivalent activity compared to the standard drug miconazole against *F. oxysporum* with MIC = 25 µg/mL. For the fungal strain *Aspergillus flavus*, compounds **7a**, **7c**, **7i** and **7j** exhibited moderate antifungal activity with MIC = 25 µg/mL in comparison with miconazole. It is surprising to note that only compound **7i** exhibited excellent antifungal activity against *Cryptococcus neoformans* with MIC = 12.5 µg/mL, and was found to be more potent than miconazole. Compounds **7a** and **7b** exhibited equipotent activity compared to the standard drug miconazole against *C. neoformans* with MIC = 25 µg/mL. Among the series, compounds bearing 4-Me, 4-OMe, 3-$NO_2$ and 2-$NO_2$ substituents on the phenyl ring exhibited excellent antifungal activity (MIC = 12.5–25 µg/mL) in comparison with the substituents 3-OMe, 2-OMe, 4-Cl, 3-Cl and 4-$NO_2$.

## Antioxidant activity

Antioxidant activity of all the synthesized compounds **7a–j** was measured against 2,2-diphenyl-1-picrylhydrazyl (DPPH). DPPH radical scavenging assay is the most commonly utilized method for screening antioxidant activity of natural as well as synthetic oxidants. Radical scavenging activity was measured in terms of $IC_{50}$ value. Radical scavenging activity of all the compounds was evaluated in comparison with BHT, and the results are summarized in Table 3. It was observed that among the

series, most of the compounds exhibited excellent radical scavenging activities with promising lower $IC_{50}$ values in comparison with BHT. Compounds **7a**, **7c**, **7e**, **7f** and **7j** exhibited potent antioxidant activity with lower $IC_{50}$ values of 15.54 ± 0.11, 12.47 ± 0.60, 15.63 ± 0.81, 15.38 ± 0.27 and 16.49 ± 0.44 µg/mL, respectively, in comparison with BHT. Compounds **7b**, **7d**, **7g**, **7h** and **7i** exhibited $IC_{50}$ values of 19.19 ± 0.47, 40.09 ± 0.29, 17.84 ± 0.90, 18.03 ± 0.92 and 21.39 ± 0.71 µg/mL, respectively. These results indicate that both electron-donating and electron-withdrawing groups present at the meta position of the phenyl ring lower the antioxidant activity.

## Computational study

### Molecular docking

In an effort to elucidate the possible mechanism by which the title compounds can induce antifungal activity and guide further structure–activity relationship (SAR) studies, molecular docking was performed in the active site of a crucial fungal target-sterol 14α-demethylase (CYP51) inhibition which prevents the conversion of lanosterol to ergosterol and subsequent accumulation of 14α-methyl sterols in the cell leading to impaired cell growth in fungi. This in silico approach has now become an integral part of the drug discovery pipeline, especially in the absence of available resources to carry out the enzymatic assays, imparting knowledge on binding affinities, binding modes and the associated thermodynamic interactions with the target enzyme governing the inhibition of the causative pathogen. It is observed that all the ligands (**7a**–**7j**) showed similar orientation in the CYP51 active site, and their complex formed was stabilized by formation of several bonded and non-bonded interactions. Even their binding energies signifying the binding affinity were observed to be negative (-48.42 to -34.22 kcal/mol) while the average docking score was seen to be -7.494 kcal/mol. An in-depth investigation of the per-residue interaction between these compounds and the residues in the active site of the enzyme has been carried out to identify the most prominently interacting residues and their type of thermodynamic interactions (bonded and non-bonded interactions) that are critical in lead optimization. This analysis is discussed in detail for the most active 1,2,3-triazole-linked tetrahydrobenzo[*b*]pyran derivative (**7c**), and the results are summarized in Table 4 for the remaining molecules in the series.

**Table 4 Quantitative per-residue interaction analysis of the molecular docking study on sterol 14α-demethylase (CYP51) for the 1,2,3-triazole-linked tetrahydrobenzo[*b*]pyran derivatives**

Visual inspection and per-residue interaction analysis for the lowest energy docked conformation of

these analogues, **7c**, showed that they could snugly fit into the active site of CYP51 at the same coordinates as the native ligand with a significantly higher binding affinity (docking score of −9.021 and GLIDE binding energy of −48.42 kcal/mol) engaging in a series of steric and electrostatic interactions (Fig. 4).

**Fig. 4**

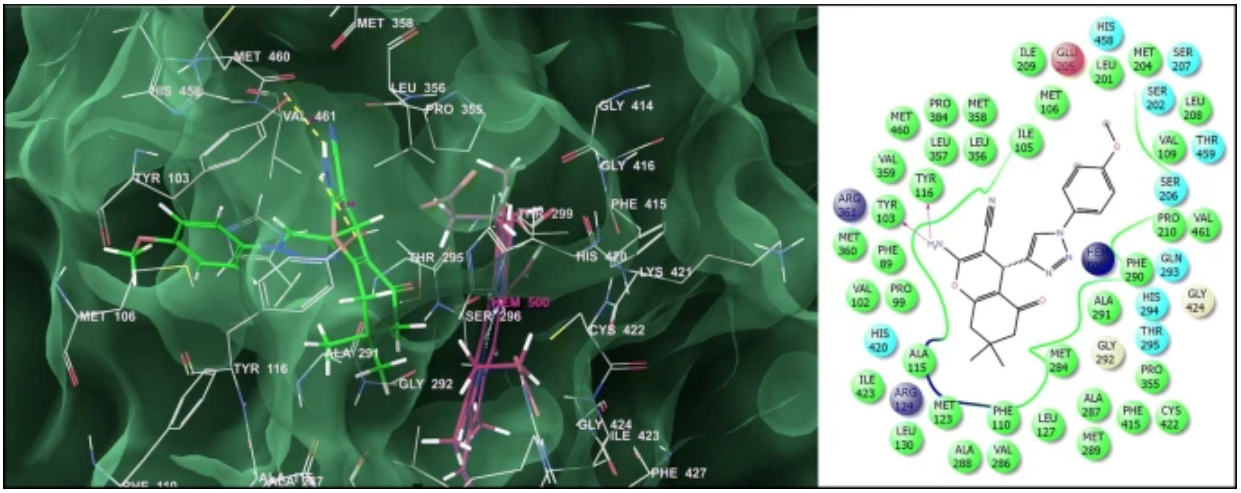


Binding mode of **7c** into the active site of sterol 14α-demethylase (CYP51) (on right side: green lines signify $\pi-\pi$ stacking interactions while the pink lines represent the hydrogen bonding interactions)

Compound **7c** was observed to be stabilized in the active site of CYP51 through a series of significant van der Waals and electrostatic interactions. However, the most noticeable hydrogen bonding interactions are of the amino ($NH_2$) on the pyran ring of **7c** with Tyr103 (2.11 Å) and Tyr116 (2.64 Å) residues. Such hydrogen bonding and $\pi-\pi$ stacking interactions serve as an anchor for guiding the orientation of the ligand in the 3D space of active sites and facilitate the non-bonded (steric and electrostatic) interactions for the stabilizing the enzyme-inhibitor complex. Furthermore, **7c** was found to be engaged in a series of significant van der Waals interactions with residues lining the active site of CYP51; for **7c** with Hem500 (−6.921 kcal/mol), Val461 (−2.104 kcal/mol), His294 (−1.934 kcal/mol), Ala291 (−2.381 kcal/mol), Phe290 (−2.011 kcal/mol), Leu208 (−2.365 kcal/mol) and Glu205 (−1.694 kcal/mol) through the 2-amino-4-1-(4-methoxyphenyl)-1*H*-1,2,3-triazol-4-yl component, while the 7,7-dimethyl-5-oxo-5,6,7,8-tetrahydro-4*H*-chromene-3-carbonitrile component got engaged in similar interactions with Met460 (−2.018 kcal/mol), Val359 (−1.993 kcal/mol), Leu356 (−2.585 kcal/mol), Thr295 (−1.683 kcal/mol), Tyr116 (−2.111 kcal/mol), Phe110 (−1.886 kcal/mol) and Met106 (−2.354 kcal/mol) residues around active site. The higher binding observed for **7c** is also attributed to a relatively fewer but significant electrostatic interactions. **7c** was observed to be engaged

in set of interactions with Hem500 (-4.298 kcal/mol), Thr295 (-1.179 kcal/mol) and Tyr103 (-1.654 kcal/mol) residues stabilizing the enzyme-inhibitor complexes. A similar network of bonded and non-bonded interactions was involved in stabilizing other molecules of the series into the active site CYP51 (Figs. 1S–9S, Supplementary Information). Furthermore, it is noteworthy that all the molecules in the series were seen to be engaged in very strong van der Waals as well as electrostatic interactions with the Heme moiety present in the active site of CYP51, which is an important observation considering the fact that fluconazole is as well coordinated in the active site of CYP51 through the iron metal, indicating that the title compounds may also share a similar mechanism for their anti-fungal action as fluconazole. Overall, the information derived from the per-residue ligand interaction analysis could be fruitfully utilized for the structure-based lead optimization to arrive at potent antifungal agents with this scaffold.

### In silico ADME prediction

A drug is said to be successful not only due to its oral bioavailability but also due to the good adsorption, distribution, metabolism and excretion (ADME). Recently, Reddyrajula et al. [59] reported in silico ADME studies of phenothiazine incorporating 1,2,3-triazole hybrids. For the prediction of ADME properties, we have calculated molecular volume (MV), molecular weight (MW), log of partition coefficient (mi log *p*), number of hydrogen bond donors (*n*-ON), number of hydrogen bond acceptors (*n*-OHNH), topological polar surface area (TPSA), number of rotatable bonds (*n*-ROTB) and Lipinski's rule of five [60] using the Molinspiration online property calculation toolkit [61]. Absorption (% ABS) was calculated by the formula % ABS = 109 - (0.345 × TPSA) [62]. The results of ADME prediction are summarized in Table 5. It is observed that the compounds exhibited good absorption (% ABS) ranging between 40 and 72%. Moreover, most of the compounds show good agreement with Lipinski's rule of five. The drug likeness model score, a collective property of physico-chemical properties, was also calculated by using MolSoft software [63]. Thus, from the observations, it was found that most of the derivatives have the potential to be developed as orally active drug-like molecules and may be lead compounds as antifungal and antioxidant drug candidates.

**Table 5 Pharmacokinetic parameters of the compounds 7a–j using in silico ADME prediction**

## Conclusions

A convenient protocol was designed for the synthesis of new 1,2,3-triazoles bearing a

tetrahydrobenzo[*b*]pyran ring using $NaHCO_3$ under ultrasonic irradiation and their biological evaluation. In vitro antifungal assay showed the compounds **7b**, **7c**, **7i** and **7j** exhibited excellent antifungal activity (MIC = 12.5 µg/mL). Among the series, most of the compounds exhibited more potent antioxidant activity than BHT with a lower $IC_{50}$ value. Molecular docking studies against a target enzyme, sterol 14α-demethylase (CYP51), showed significant correlation between binding score and antifungal activity. We can conclude that 1,2,3-triazole-bearing tetrahydrobenzo[*b*]pyran derivatives could be promising lead compounds for the development of new antifungal and antioxidant agents in clinical research.

## References

1. Y. Wang, J. Xie, Y. Xing, L. Chen, Y. Li, T. Meng, W. Dong, X. Wang, Y. Dong, Antimicrob. Agents Chemother. **61**, e00620-17 (2017)

Article PubMed PubMed Central Google Scholar

2. C.Y. Low, C. Rotstein, F1000 Med. Rep. **3**, 14 (2011)

Article PubMed PubMed Central Google Scholar

3. M.K. Kathiravan, A.B. Salake, A.S. Chothe, P.B. Dudhe, R.P. Watode, M.S. Mukta, S. Gadhwe, Bioorg. Med. Chem. **20**, 5678 (2012)

Article CAS PubMed Google Scholar

4. L. Scorzoni, A.C. de Paula, E. Silva, C.M. Marcos, P.A. Assato, W.C. de Melo, H.C. de Oliveira, C.B. Costa-Orlandi, M.J. Mendes-Giannini, A.M. Fusco-Almeida, Front. Microbiol. **8**, 36 (2017)

Article PubMed PubMed Central Google Scholar

5. V.T. Andriole, Int. J. Antimicrob. Agents **16**, 317 (2000)

Article CAS PubMed Google Scholar

6. J. Beardsley, C.L. Halliday, S.C. Chen, T.C. Sorrell, Future Microbiol. **13**, 1175 (2018)

Article CAS PubMed PubMed Central Google Scholar

7. T.Y. Hargrove, Z. Wawrzak, J. Liu, M.R. Waterman, W.D. Nes, G.I. Lepesheva, J. Lipid Res. **53**, 311 (2012)

Article CAS PubMed PubMed Central Google Scholar

8. K. Xu, L. Huang, Z. Xu, Y. Wang, G. Bai, Q. Wu, X. Wang, S. Yu, Y. Jiang, Drug Des. Dev. Ther. **9**, 1459 (2015)

Google Scholar

9. R. Guezguez, K. Bougrin, K. El Akri, R. Benhida, Tetrahedron Lett. **47**, 4807 (2006)

Article CAS Google Scholar

10. N.D. Thanh, D.S. Hai, N.T.T. Ha, D.T. Tung, C.T. Le, H.T.K. Van, V.N. Toan, D.N. Toan, L.H. Dang, Bioorg. Med. Chem. Lett. **29**, 164 (2019)

Article CAS PubMed Google Scholar

11. F. Alonso, Y. Moglie, G. Radivoy, M. Yus, J. Org. Chem. **76**, 8394 (2011)

Article CAS PubMed Google Scholar

12. S.G. Agalave, S.R. Mauja, V.S. Pore, Chem. Asian J. **6**, 2696 (2011)

Article CAS PubMed Google Scholar

13. Z. Jiang, J. Gu, C. Wang, S. Wang, N. Liu, Y. Jiang, G. Dong, Y. Wang, Y. Liu, J. Yao, Z. Miao, W. Zhang, C. Sheng, Eur. J. Med. Chem. **82**, 490 (2014)

Article CAS PubMed Google Scholar

14. C. Gill, G. Jadhav, M. Shaikh, R. Kale, A. Ghawalkar, D. Nagargoje, M. Shiradkar, Bioorg. Med.

Chem. Lett. **18**, 6244 (2008)

Article CAS PubMed Google Scholar

15. J. Mareddy, N. Suresh, C.G. Kumar, R. Kapavarapu, A. Jayasree, S. Pal, Bioorg. Med. Chem. Lett. **27**, 518 (2017)

Article CAS PubMed Google Scholar

16. R. Pratap, V.J. Ram, Chem. Rev. **114**, 10476 (2014)

Article CAS PubMed Google Scholar

17. D. Kumar, V.B. Reddy, S. Sharad, U. Dube, S. Kapur, Eur. J. Med. Chem. **44**, 3805 (2009)

Article CAS PubMed Google Scholar

18. R.R. Kumar, S. Perumal, J.C. Menendez, Y. Perumal, D. Sriram, Bioorg. Med. Chem. **19**, 3444 (2011)

Article CAS Google Scholar

19. A.M. Shestopalov, Y.M. Litvinov, L.A. Rodinovskaya, O.R. Malyshev, M.N. Semenova, V.V. Semeno, ACS Comb. Sci. **14**, 484 (2012)

Article CAS PubMed Google Scholar

20. N.M. Sabry, H.M. Mohamed, E.S.A.E.H. Khattab, S.S. Motlaq, A.M. El-Agrody, Eur. J. Med. Chem. **46**, 765 (2011)

Article CAS PubMed Google Scholar

21. B.F. Mirjalili, L. Zamani, K. Zomorodian, S. Khabnadideh, Z. Haghighijoo, Z. Malakotikhah, S.A.A. Mousavi, S. Khojasteh, J. Mol. Struct. **1116**, 102 (2016)

Article CAS Google Scholar

22. W. Kemnitzer, J. Drewe, S. Jiang, H. Zhang, J. Zhao, C. Crogan-Grundy, L. Xu, S. Lamothe, H. Gourdeau, R. Denis, B. Tseng, S. Kasibhatla, S.X. Cai, J. Med. Chem. **50**, 2858 (2007)

Article CAS PubMed Google Scholar

23. B.M. Chougala, S. Samundeeswari, M. Holiyachi, L.A. Shastri, S. Dodamani, S. Jalalpure, S.R. Dixit, S.D. Joshi, V.A. Sunagar, Eur. J. Med. Chem. **125**, 101 (2017)

Article CAS PubMed Google Scholar

24. V.F. De Andrade-Neto, M.O. Goulart, J.F. Da Silva Filho, M.J. Da Silva, M.D.C. Pinto, A.V. Pinto, M.G. Zalis, L.H. Carvalho, A.U. Krettli, Bioorg. Med. Chem. Lett. **14**, 1145 (2004)

Article CAS PubMed Google Scholar

25. N.D. Thanh, D.S. Hai, V.T.N. Bich, P.T.T. Hien, N.T.K. Duyen, N.T. Mai, T.T. Dung, V.N. Toan, H.T.K. Van, L.H. Dang, D.N. Toan, T.T.T. Van, Eur. J. Med. Chem. **167**, 454 (2019)

Article CAS PubMed Google Scholar

26. F.N. Sadeh, M.T. Maghsoodlou, N. Hazeri, M. Kangani, Res. Chem. Intermed. **41**, 5907 (2015)

Article CAS Google Scholar

27. J. Lu, X.W. Fu, G. Zhang, C. Wang, Res. Chem. Intermed. **42**, 417 (2016)

Article CAS Google Scholar

28. I.A. Azath, P. Puthiaraj, K. Pitchumani, ACS Sustain. Chem. Eng. **1**, 174 (2013)

Article CAS Google Scholar

29. H.R. Safaei, M. Shekouhy, S. Rahmanpur, A. Shirinfeshan, Green Chem. **14**, 1696 (2012)

Article CAS Google Scholar

30. B. Amirheidari, M. Seifi, M. Abaszadeh, Res. Chem. Intermed. **42**, 3413 (2016)

Article CAS Google Scholar

31. R.S. Bhosale, C.V. Magar, K.S. Solanke, S.B. Mane, S.S. Choudhary, R.P. Pawar, Synth. Commun. **37**, 4353 (2007)

Article CAS Google Scholar

32. K.S. Pandit, P.V. Chavan, U.V. Desai, M.A. Kulkarni, P.P. Wadgaonkar, New J. Chem. **39**, 4452 (2015)

Article CAS Google Scholar

33. H. Zhi, C. Lu, Q. Zhang, J. Luo, Chem. Commun. (2009). https://doi.org/10.1039/B822481A

Article Google Scholar

34. J.A. Makawana, D.C. Mungra, M.P. Patel, R.G. Patel, Bioorg. Med. Chem. Lett. **21**, 6166 (2011)

Article CAS PubMed Google Scholar

35. M. Esmaeilpour, J. Javidi, F. Dehghani, F.N. Dodeji, RSC Adv. **5**, 26625 (2015)

Article CAS Google Scholar

36. M.G. Dekamin, M. Eslami, Green Chem. **16**, 4914 (2014)

Article CAS Google Scholar

37. O.H. Qareaghaj, S. Mashkouri, M.R. Naimi-Jamal, G. Kaupp, RSC Adv. **4**, 48191 (2014)

Article CAS Google Scholar

38. P. Anastas, N. Eghbali, Chem. Soc. Rev. **39**, 301 (2010)

Article CAS PubMed Google Scholar

39. A. Domling, I. Ugi, Angew. Chem. Int. Ed. **39**, 3168 (2000)

Article CAS Google Scholar

40. L. Levi, T.J.J. Muller, Chem. Soc. Rev. **45**, 2825 (2016)

Article CAS PubMed Google Scholar

41. M.-O. Simon, C.-J. Li, Chem. Soc. Rev. **41**, 1415 (2012)

Article CAS PubMed Google Scholar

42. G. Cravotto, P. Cintas, Chem. Soc. Rev. **35**, 180 (2006)

Article CAS PubMed Google Scholar

43. M.H. Shaikh, D.D. Subhedar, L. Nawale, D. Sarkar, F.A.K. Khan, J.N. Sangshetti, B.B. Shingate, Med. Chem. Commun. **6**, 1104 (2015)

Article CAS Google Scholar

44. D.D. Subhedar, M.H. Shaikh, B.B. Shingate, L. Nawale, D. Sarkar, V.M. Khedkar, Med. Chem. Commun. **7**, 1832 (2016)

Article CAS Google Scholar

45. D.D. Subhedar, M.H. Shaikh, L. Nawale, D. Sarkar, V.M. Khedkar, B.B. Shingate, Bioorg. Med. Chem. Lett. **27**, 922 (2017)

Article CAS PubMed Google Scholar

46. D.D. Subhedar, M.H. Shaikh, B.B. Shingate, L. Nawale, D. Sarkar, V.M. Khedkar, F.A.K. Khan, J.N. Sangshetti, Eur. J. Med. Chem. **125**, 385 (2017)

Article CAS PubMed Google Scholar

47. C. Viegas-Junior, A. Danuello, V. da Silva Bolzani, E.J. Barreiro, C.A. Fraga, Curr. Med. Chem. **14**, 1829 (2007)

Article CAS PubMed Google Scholar

48. C.H. Collins, *Microbiological Methods*, 4th edn. (Butterworth's, London, 1976)

Google Scholar

49. M. Burits, F. Bucar, Phytother. Res. **14**, 323 (2000)

Article CAS PubMed Google Scholar

50. R.A. Friesner, R.B. Murphy, M.P. Repasky, L.L. Frye, J.R. Greenwood, T.A. Halgren, P.C. Sanschagrin, D.T. Mainz, J. Med. Chem. **49**, 6177 (2006)

Article CAS PubMed Google Scholar

51. http://www.rcsb.org/pdb

52. A.B. Danne, A.S. Choudhari, D. Sarkar, J.N. Sangshetti, V.M. Khedkar, B.B. Shingate, Res. Chem. Intermed. **44**, 6283 (2018)

Article CAS Google Scholar

53. S.P. Khare, T.R. Deshmukh, J.N. Sangshetti, V.S. Krishna, D. Sriram, V.M. Khedkar, B.B. Shingate, Chem. Sel. **3**, 13113 (2018)

CAS Google Scholar

54. A.B. Danne, A.S. Choudhari, S. Chakraborty, D. Sarkar, V.M. Khedkar, B.B. Shingate, Med. Chem. Commun. **9**, 1114 (2018)

Article CAS Google Scholar

55. J.M. Khurana, S. Kumar, Tetrahedron Lett. **50**, 4125 (2009)

Article CAS Google Scholar

56. L. Ronchin, A. Vavasori, E. Amadio, G. Cavinato, L. Toniolo, J. Mol. Catal. A: Chem. **298**, 23 (2009)

Article CAS Google Scholar

57. A. Mobinikhaledi, M.A.B. Fard, Acta Chim. Slov. **57**, 931 (2010)

CAS PubMed Google Scholar

58. C. Kurumurthy, R.N. Kumar, T. Yakaiah, P.S. Rao, B. Narsaiah, Res. Chem. Intermed. **41**, 3193 (2015)

Article CAS Google Scholar

59. R. Reddyrajula, U. Dalimba, S.M. Kumar, Eur. J. Med. Chem. **168**, 263 (2019)

Article CAS PubMed Google Scholar

60. C.A. Lipinski, F. Lombardo, B.W. Dominy, P.J. Feeney, Adv. Drug Deliv. Rev. **46**, 3 (2001)

Article CAS PubMed Google Scholar

61. http://www.molinspiration.com/cgibin/properties (2014)

62. Y.H. Zhao, M.H. Abraham, J. Le, A. Hersey, C.N. Luscombe, G. Beck, B. Sherborne, I. Cooper, Pharm. Res. **19**, 1446 (2002)

Article CAS PubMed Google Scholar

63. http://www.molsoft.com/mprop

## Acknowledgements

One of the authors, S.P.K., is grateful to Dr. Babasaheb Ambedkar Marathwada University, Aurangabad, for the award of university scholars fellowship. The authors are also thankful to the Head, Department of Chemistry, Dr. Babasaheb Ambedkar Marathwada University, Aurangabad, 431 004, India, for providing the laboratory facility. The authors are also thankful to Schrodinger Inc. for providing the Schrodinger molecular modeling software for performing the molecular studies.

## Author information

### Authors and Affiliations

**Department of Chemistry, Dr. Babasaheb Ambedkar Marathwada University, Aurangabad, 431 004, India**
Smita P. Khare, Tejshri R. Deshmukh, Satish V. Akolkar & Bapurao B. Shingate

**Department of Pharmaceutical Chemistry, Y. B. Chavan College of Pharmacy, Dr. Rafiq Zakaria Campus, Aurangabad, 431 001, India**
Jaiprakash N. Sangshetti

**Department of Pharmaceutical Chemistry, Shri Vile Parle Kelavani Mandal's Institute of Pharmacy, Dhule, 424 001, India**
Vijay M. Khedkar

### Corresponding author

Correspondence to Bapurao B. Shingate.

## Additional information

## Publisher's Note



## Electronic supplementary material

Below is the link to the electronic supplementary material.

## Supplementary material 1 (PDF 3153 kb)

## Rights and permissions



## About this article

### Cite this article

Khare, S.P., Deshmukh, T.R., Akolkar, S.V. *et al.* New 1,2,3-triazole-linked tetrahydrobenzo[*b*]pyran derivatives: Facile synthesis, biological evaluation and molecular docking study. *Res Chem Intermed* **45**, 5159–5182 (2019). https://doi.org/10.1007/s11164-019-03906-0

| Received | Accepted | Published |
| --- | --- | --- |
| 05 February 2019 | 14 June 2019 | 21 June 2019 |

Issue Date
October 2019

DOI
https://doi.org/10.1007/s11164-019-03906-0

### Share this article

## Keywords

1,2,3-Triazole Tetrahydrobenzo[*b*]pyran Multicomponent reactions

Antifungal activity Molecular docking study